Cell

Genome-wide Analysis Reveals MOF as a Key Regulator of Dosage Compensation and Gene Expression in *Drosophila*

Jop Kind,[1,3] Juan M. Vaquerizas,[2,3] Philipp Gebhardt,[1] Marc Gentzel,[1] Nicholas M. Luscombe,[1,2] Paul Bertone,[1,2] and Asifa Akhtar[1,*]

[1]Gene Expression Unit, European Molecular Biology Laboratory, Meyerhofstrasse 1, 69117 Heidelberg, Germany
[2]EMBL European Bioinformatics Institute, Wellcome Trust Genome Campus, Cambridge CB10 1SD, UK
[3]These authors contributed equally to this work.
*Correspondence: akhtar@embl.de
DOI 10.1016/j.cell.2008.04.036

SUMMARY

Dosage compensation, mediated by the MSL complex, regulates X-chromosomal gene expression in *Drosophila*. Here we report that the histone H4 lysine 16 (H4K16) specific histone acetyltransferase MOF displays differential binding behavior depending on whether the target gene is located on the X chromosome versus the autosomes. More specifically, on the male X chromosome, where MSL1 and MSL3 are preferentially associated with the 3′ end of dosage compensated genes, MOF displays a bimodal distribution binding to promoters and the 3′ ends of genes. In contrast, on MSL1/MSL3 independent X-linked genes and autosomal genes in males and females, MOF binds primarily to promoters. Binding of MOF to autosomes is functional, as H4K16 acetylation and the transcription levels of a number of genes are affected upon MOF depletion. Therefore, MOF is not only involved in the onset of dosage compensation, but also acts as a regulator of gene expression in the *Drosophila* genome.

INTRODUCTION

Genetic material does not exist freely in the cell but is in complex with histone proteins to form chromatin. Histones are subject to a wide variety of posttranslational modifications that impose changes on chromatin structure. Among the various histone modifications, acetylation is one of the best studied (for reviews see (Kurdistani and Grunstein, 2003; Lee and Workman, 2007; Yang and Seto, 2007). X-chromosomal dosage compensation in *Drosophila melanogaster* is a model system that is used to gain better understanding of broad chromosome-wide transcriptional regulation by hyperacetylation *(*for reviews see Lucchesi et al., 2005; Mendjan and Akhtar, 2006; Straub and Becker, 2007).

Dosage compensation is a process that balances the expression of sex-linked genes in species that have evolved unequal numbers of sex chromosomes. In *Drosophila* this involves hyperactivation of the single male X chromosome to equalize for the combined transcriptional activity of both female X chromosomes. This process is regulated by the MSL complex, which consists of at least five male-specific lethal proteins (MSL1, MSL2, MSL3, *m*ale*l*ess [MLE], and *m*ales-absent-*o*n-the-*f*irst [MOF]) and two noncoding RNAs (roX1 and roX2) (for review see Straub and Becker, 2007).

Although the individual components of the MSL complex have been studied extensively, the molecular mechanisms underlying the process of dosage compensation remain poorly characterized. MSLs are thought to function, in part, in the recruitment and activation of MOF at the X chromosome. MOF is a histone acetyl transferase (HAT) that specifically acetylates lysine 16 of histone H4 (H4K16Ac), a modification found highly enriched on the male X chromosome (Akhtar and Becker, 2000; Bone et al., 1994; Hilfiker et al., 1997; Smith et al., 2000).

The role of H4K16Ac in transcriptional regulation is not completely understood. *Drosophila* MOF protein targeted to a heterologous promoter by the GAL4 DNA-binding domain releases chromatin-mediated transcriptional repression by H4K16Ac in yeast (Akhtar and Becker, 2000) and causes chromatin decondensation on the male X chromosome in *Drosophila* (Corona et al., 2002). Although H4K16Ac does not correlate with active genes in yeast (Kurdistani et al., 2004), it is specifically associated with the activity of a subset of genes, whereas all other acetylation marks on histone H4 exhibit an additive effect (Dion et al., 2005). H4K16Ac modifications pose a structural constraint on higher-order chromatin formation; it is therefore possible that maintenance of transcriptional potential could be one of its functions. In this role, H4K16Ac would serve to limit the association of repressive protein complexes and, in tandem, relax the chromatin fiber to permit accessibility of the transcriptional machinery (Shogren-Knaak et al., 2006). At present, the distribution of H4K16Ac across the length of gene loci, together with its presumed role in chromatin decondensation, has given rise to the hypothesis that the MSL complex is involved in transcriptional elongation (Smith et al., 2001).

Although MSLs are mainly studied in *Drosophila,* all MSL proteins have conserved orthologs in mammals (Marin, 2003). This implies functional conservation in species with radically different dosage compensation mechanisms. Not only do the human

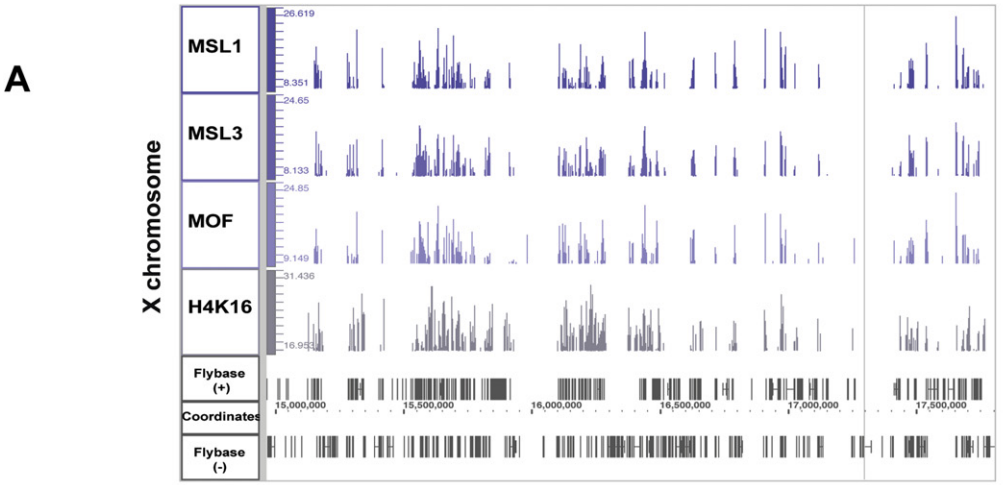
A
X chromosome
MSL1
MSL3
MOF
H4K16
Flybase (+)
Coordinates
Flybase (-)
15,000,000
15,500,000
16,000,000
16,500,000
17,000,000
17,500,000

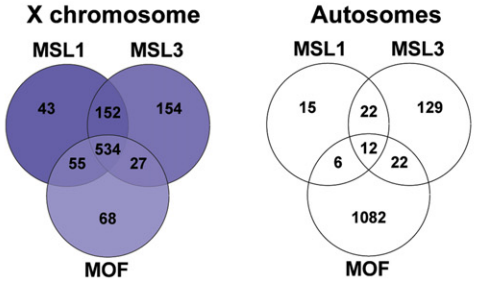
B
X chromosome
MSL1
MSL3
43
152
154
534
55
27
68
MOF
Autosomes
MSL1
MSL3
15
22
129
12
6
22
1082
MOF

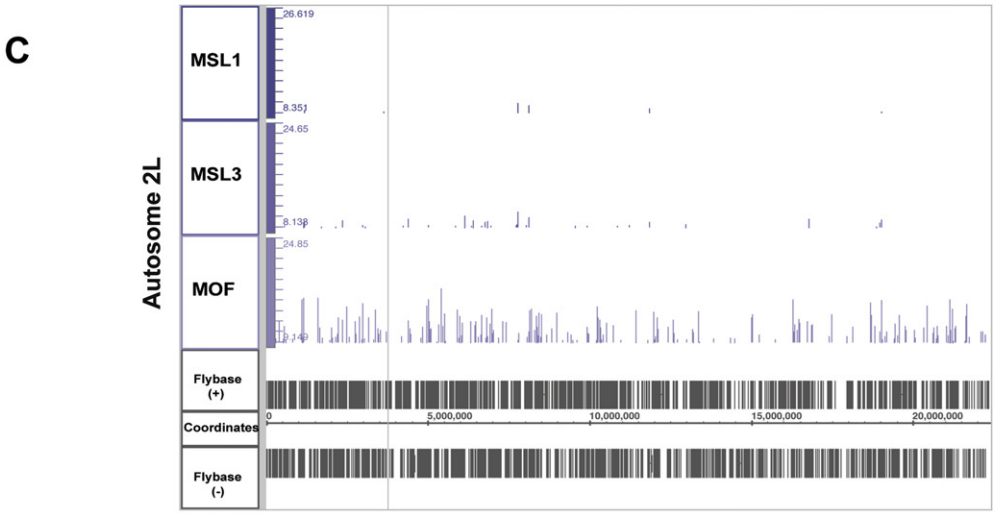
C
Autosome 2L
MSL1
MSL3
MOF
Flybase (+)
Coordinates
Flybase (-)
0
5,000,000
10,000,000
15,000,000
20,000,000

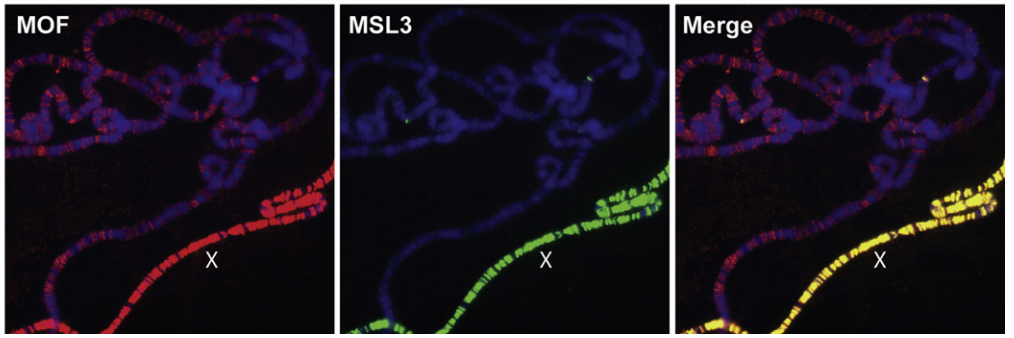
D
MOF
MSL3
Merge
X
X
X

MSLs (hMSL) form a complex like in *Drosophila*, most of their interaction partners are also conserved (Mendjan et al., 2006; Smith et al., 2005; Taipale et al., 2005). Furthermore, MOF in *Drosophila* is the only MSL protein to bind all chromosomes independently of the MSL complex in both males and females (Bhadra et al., 1999). These properties, together with evidence of evolutionary conservation, suggest a role for both MOF and H4K16Ac in transcriptional regulation beyond the process of dosage compensation.

To gain insight into the role of MOF in the regulation of gene expression, we performed a comprehensive genome-wide analysis of MOF/MSL-bound DNA by a series of chromatin immunoprecipitations directed against specific MSL proteins, followed by hybridization to high-resolution tiling arrays (the ChIP-chip method; see Horak and Snyder, 2002). This strategy allowed us to generate binding profiles for MSL1, MSL3, and MOF, along with H4K16 acetylation, in "male" Schneider (SL-2) cells as well as MOF and H4K16Ac in "female" Kc cells (see below). These analyses were complemented with microarray-based gene expression profiles of SL-2 cells depleted of MSL1, MSL3, and MOF, and of MOF-depleted Kc cells.

Our data reveal MOF as a transcriptional regulator, not only on the X chromosome but also on autosomes. Intriguingly, MOF on the X chromosome associates with promoters and the 3′ end of genes, whereas on autosomes and the female genome MOF associates primarily with promoters. Furthermore, an accumulation of H4K16Ac marks is observed over entire gene loci on the X chromosome, whereby this pattern is a direct reflection of MOF activity, while on autosomes, acetylation was found to peak toward the 5′ end of target genes. Interestingly, we found that binding to 3′ ends of genes by MSL1, MSL3, and MOF is interdependent on the X chromosome; however, MOF association to promoter-proximal regions was found to be independent of MSL1, similar to the binding site distribution across the autosomes. It therefore appears that the role of the MSL complex members is to recruit MOF toward the gene interior, allowing more extended acetylation toward the 3′ end. These results provide interesting insights into the mechanism of MSL complex recruitment on dosage-compensated genes and reveal an unprecedented role of MOF on autosomes independent of the MSL complex.

RESULTS

Correlated MSL Binding and H4K16 Acetylation on the Male X Chromosome

We created high-resolution (35 bp) genome-wide DNA-binding profiles of MSL1, MSL3, MOF, and H4K16Ac in *Drosophila* Schneider SL-2 cells using the ChIP-chip method to hybridize chromatin-immonuprecipitated DNA to Affymetrix tiling arrays. To equalize for the level of histones, control ChIP samples were isolated using a histone H4 specific antibody. ChIP DNA samples were produced and hybridized as three independent biological replicates, which showed highly reproducible binding profiles (Figures S1 and S2). To facilitate unbiased comparisons across different ChIP-chip experiments, we considered the topmost one percent of enriched binding-site loci scored for each condition (see Experimental Procedures).

The use of genome-wide tiling arrays makes it possible to study the localization of MSL1, MSL3, MOF, and H4K16Ac sites systematically, on all chromosomes and at high resolution. To elucidate the properties of DNA association independently of dosage compensation, we analyzed binding-site occupancy of each protein over the X chromosome and the autosomes in parallel. Chromatin profiling of MSL1, MSL3, MOF, as well as H4K16 acetylation exhibited a high degree of coincidence across the X chromosome (Figure 1A). As expected, we observed a clear preference for MSL1, MSL3, and MOF to bind the X chromosome rather than autosomes (Figure S3). Further analysis revealed that 534 X-chromosomal genes were bound by the three MSL proteins (Figure 1B).

To further assess the accuracy of our approach, we examined a large (~150 kb) region of the X chromosome for binding of MSL1 and MOF with three independent chromatin samples followed by quantitative real-time PCR (qRT-PCR). In addition, primers were designed to amplify the *roX2* and *runt* genes; these serve as positive and negative controls, respectively, and have been used routinely for this purpose in other studies of the MSL complex (Kind and Akhtar, 2007; Legube et al., 2006; Smith et al., 2001). These qRT-PCR results correlate well with the profiles generated by global ChIP-chip analyses (Figure S4).

MSL1 and MSL3 are bound to few autosomal genes, whereas MOF displayed extensive binding to autosomes (Figures 1B, 1C, and S5). Consistent with these observations, MOF was also found to associate globally to autosomes on polytene chromosomes, albeit with a clearly lower incidence of binding than on the X chromosome (Figure 1D). In contrast to MOF, only a small number of sites could be observed for MSL3 on autosomes (Figure 1D). We therefore conclude that in contrast to MSL1 and MSL3, which preferentially bind to the X chromosome, MOF also binds extensively to autosomes.

MOF Displays a Bimodal Binding Pattern on X-Chromosomal Genes

As demonstrated here, MSL1, MSL3, and MOF display a clear preference for binding to loci across the X chromosome. Given these results, we then examined individual gene components to elucidate patterns of binding to coding sequences, introns, and untranslated regions. Consistent with previous observations

Figure 1. High-Resolution Map of MSL1, MSL3, MOF, and H4K16Ac Chromatin Profiling in *Drosophila* SL-2 Cells

(A) MOF binds the X chromosome in association with the MSL complex, but binds independently to autosomes. Shown in (A) are topmost 1% ranked binding loci of MSL1, MSL3, MOF, and H4K16Ac on a section of the X chromosome representing 1.5 Mb. Flybase (+) and (−) represents the location of genes on the forward and reverse DNA strands, respectively. Coordinates represent the position on the corresponding chromosome.

(B) Overlap of MSL1, MSL3 and MOF target genes on the X chromosome and autosomes.

(C) Comparison of the distribution of MSL1, MSL3, and MOF binding on the chromosome arm 2L.

(D) Immunostaining of polytene chromosomes from male third instar larvae using antibodies against MOF (red) and MSL3 (green). DNA staining is shown in blue (Hoechst 322).

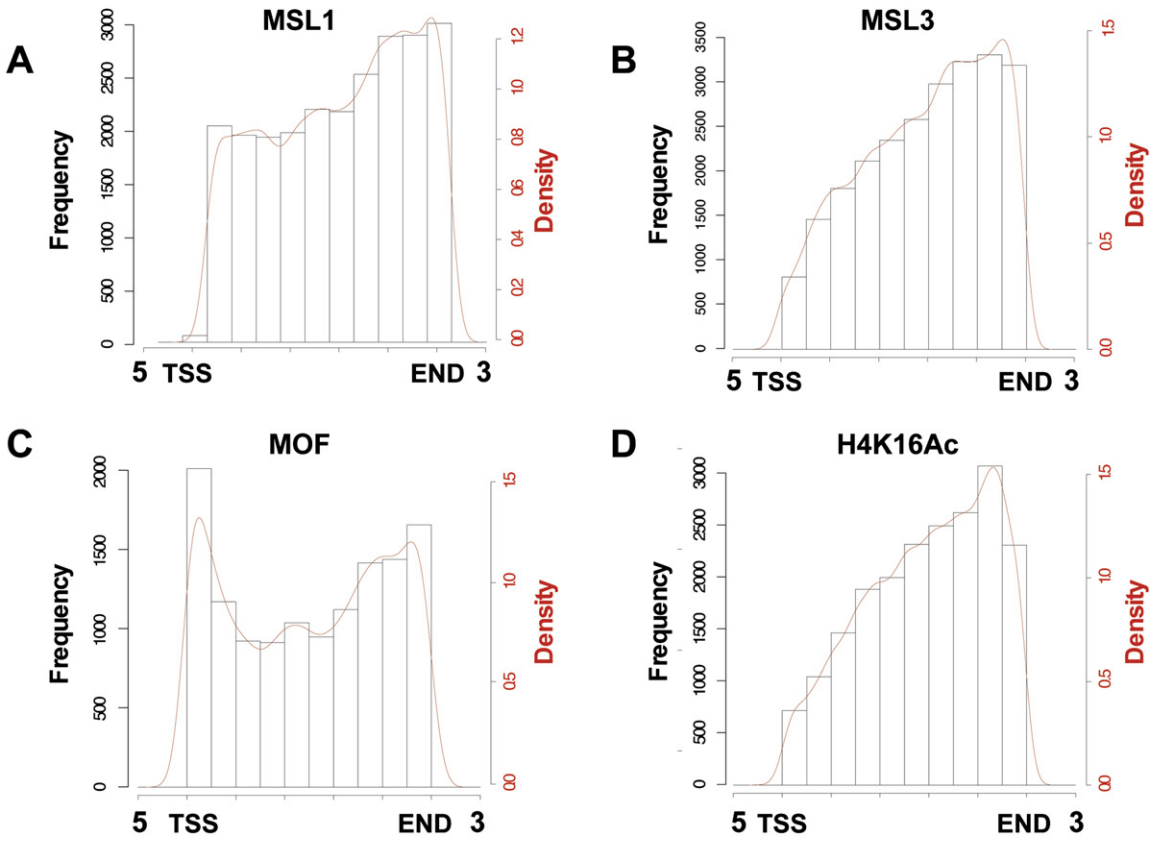
A
MSL1
Frequency
Density
5 TSS
END 3
B
MSL3
Frequency
Density
5 TSS
END 3
C
MOF
Frequency
Density
5 TSS
END 3
D
H4K16Ac
Frequency
Density
5 TSS
END 3

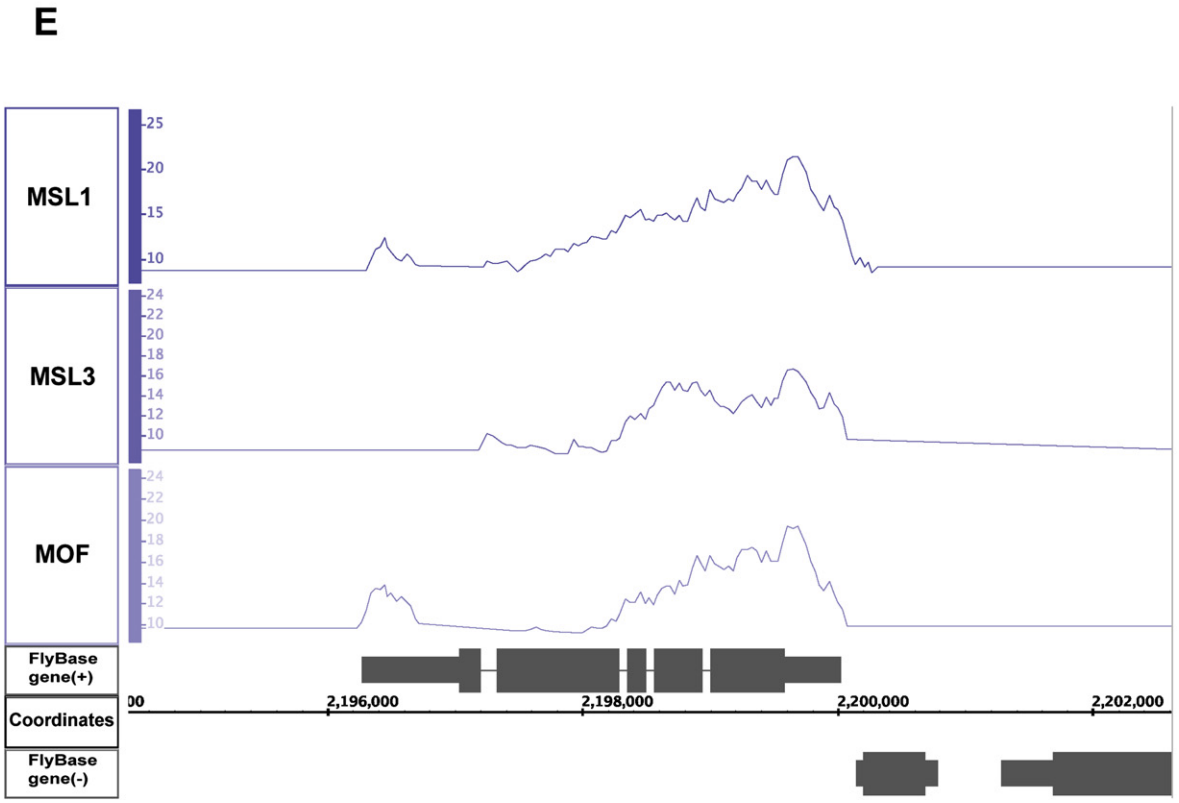
E
MSL1
MSL3
MOF
FlyBase gene(+)
Coordinates
FlyBase gene(-)
2,196,000
2,198,000
2,200,000
2,202,000

(Alekseyenko et al., 2006; Gilfillan et al., 2006; Legube et al., 2006), MSL1, MSL3, and MOF bind preferentially to gene loci over both intergenic regions and UTRs on the X chromosome (Figure S6A–S6C). In striking contrast, however, a significant enrichment of MOF binding sites to autosomal intergenic regions and 5′UTRs was observed, whereas binding to 3′UTRs is nearly absent (Figure S6C and S6E). This marked shift in binding preference suggests diversified functional association of MOF to intragenic regions between the X chromosome and autosomes.

To establish an average binding profile across regulated gene loci, oligonucleotide probe sets corresponding to bound genes (on X chromosomes and autosomes) were analyzed for relative binding frequency along the scaled lengths of gene loci (Figures 2A–2D and S7). In this manner, it can be seen that H4K16 acetylation gradually increases toward the 3′ ends of genes, similar to the pattern displayed by MSL1 and MSL3. Surprisingly however, MOF displays a bimodal pattern of binding toward the beginning and the 3′ end of genes (compare Figure 2C to Figures 2A, 2B, and 2D). Similar results were obtained by performing the analyses reporting only one significant bound probe per gene per standardized region to account for gene length effects (data not shown). Distribution of individual probe intensities across individual genes further confirmed that this bimodal binding of MOF represent the bona fide behavior of MOF on individual genes rather then a simple superimposition of two distinct classes of sites on the X chromosome (Figures 2E and S8).

Complementary analyses of MOF binding at transcription start and stop sites revealed that MOF binding peaks at promoter regions, on autosomal and X chromosomal target genes. In addition, MOF binds along the body and 3′ end of genes located on the X chromosome (Figures S9 and S10). MOF is enriched approximately 0–500 bp upstream of the transcription start site, which we refer to hereafter as MOF promoter binding (Figure S9). Intriguingly, the H4K16Ac profile across the X chromosome is enriched toward the 3′ ends of genes in a pattern very similar to the MSL3 profile (compare Figure 2B with 2D). Intensity of MOF binding at 3′ end of X-linked genes was significantly higher compared to the 5′ ends ($p < 4e-08$) (Figure S11A). In contrast, MOF binding on autosomes was significantly higher at 5′ ends of autosomal genes (p 0.014) (Figure S11B).

It therefore appears evident that in SL-2 cells MOF binds to promoters as well as throughout the body of X-chromosomal genes, where binding peak at 3′ ends. This is in contrast to the activity observed on autosomes, where MOF binding peaks at promoters.

MOF Binds Promoter-Proximal Regions in Kc Cells

Differential binding of MOF to X chromosomal genes and autosomes with respect to MSL1 and MSL3 in SL-2 cells (Figures 2C and S7C) prompted us to perform genome-wide analysis of MOF binding and H4K16Ac in Kc cells. In Kc cells, MSL2 is translationally repressed by SXL as part of the sex-determination pathway (Bashaw and Baker, 1995; Zhou et al., 1995). Consequently, the MSL complex cannot assemble, and its members are unstable (Kelley et al., 1995). Kc cells may therefore be regarded as ''female'' cells as opposed to ''male'' SL-2 cells where MSL complex members are expressed and exhibit the classical staining pattern of the male X chromosome (Duncan et al., 2006; Mendjan et al., 2006).

In contrast to the pattern of activity observed in SL-2 cells, MOF binding sites and H4K16Ac marks are not restricted to the X chromosome but rather are distributed evenly across the genome in Kc cells (Figures S3, S6E, S6F and 3A). In addition, MOF does not display a bimodal distribution across gene loci in Kc cells, but instead is mainly restricted to promoters with a concurrent shift in the H4K16Ac profile from 3′ to 5′ enrichment (Figure S9). Notably, when in SL-2 cells the top-most-ranked 1% significant autosomal gene targets were analyzed independently of the X chromosome, the MOF and H4K16Ac profiles appear nearly identical to those obtained from Kc cells (Figure 3B).

Furthermore, a significant number of genes are similarly bound by MOF on autosomes in SL-2 and Kc cells (Figure 3C). In keeping with these results, the binding-site occupancy is nearly identical between both cell types (Figure S12). Interestingly, we found that the intensity of 5′ MOF binding was significantly higher on the X chromosome versus autosomes in both SL-2 cells ($p < 2e-18$) and Kc cells ($p < 3e-08$) (Figure S13). Furthermore, MOF binding correlated highly significantly with H4K16Ac occupancy in both SL-2 ($p < 2.2e-16$) and Kc cells ($p < 2.2e-16$) (Figure 3D). We also found that approximately 80% of all MOF-bound targets (autosomes and X chromosomes) are active genes in both SL-2 and Kc cells (Figure S14; see Supplemental Experimental Procedures). Among the 1980 genes bound by MOF in the two cell lines, Gene Ontology (GO) analysis revealed a number of statistically overrepresented biological processes related to the cell cycle (Figure S14C; Table S1). Similarly, a variety of other biological processes were found to be significant among genes bound independently in either SL-2 (971 genes) or Kc cells (943 genes). These results are summarized in Tables S2 and S3.

Taken together these results demonstrate that MOF, in addition to binding across the body of genes on the male X chromosome, binds promoters of transcriptionally active genes in both SL-2 and Kc cells on all chromosomes.

MOF Binding to Promoters Is Independent of MSL1

Global analyses in both cell types revealed that MOF resides on promoters on all chromosomes (Figures 2 and 3). Invariant

Figure 2. Bimodal Distribution of MOF on X-Chromosomal Genes

(A–D) Normalized binding distribution to gene loci in SL-2 cells using topmost1% targets. Distribution of MSL1, MSL3, and MOF and H4K16Ac across the X chromosome. Genes with significant binding were scaled to similar lengths, and the relative position of significant probes was computed. Bars represent the number of significant probes in a given region. A continuous fit of the distribution is depicted in red. MOF binds to promoters (5′ ends) and toward the 3′ ends of X-chromosomal gene loci. This bimodal binding pattern is different from the primarily 3′ enrichment of MSL1, MSL3, and H4K16Ac (A-D). TSS represents (transcription start site) and END represents (transcription stop site).

(E) MSL1, MSL3, and MOF binding intensity on a single X-chromosomal target gene (PH1). Flybase (+) and (−) represents the location of genes on the forward and reverse DNA strands respectively. Coordinates represent the position on the corresponding chromosome.

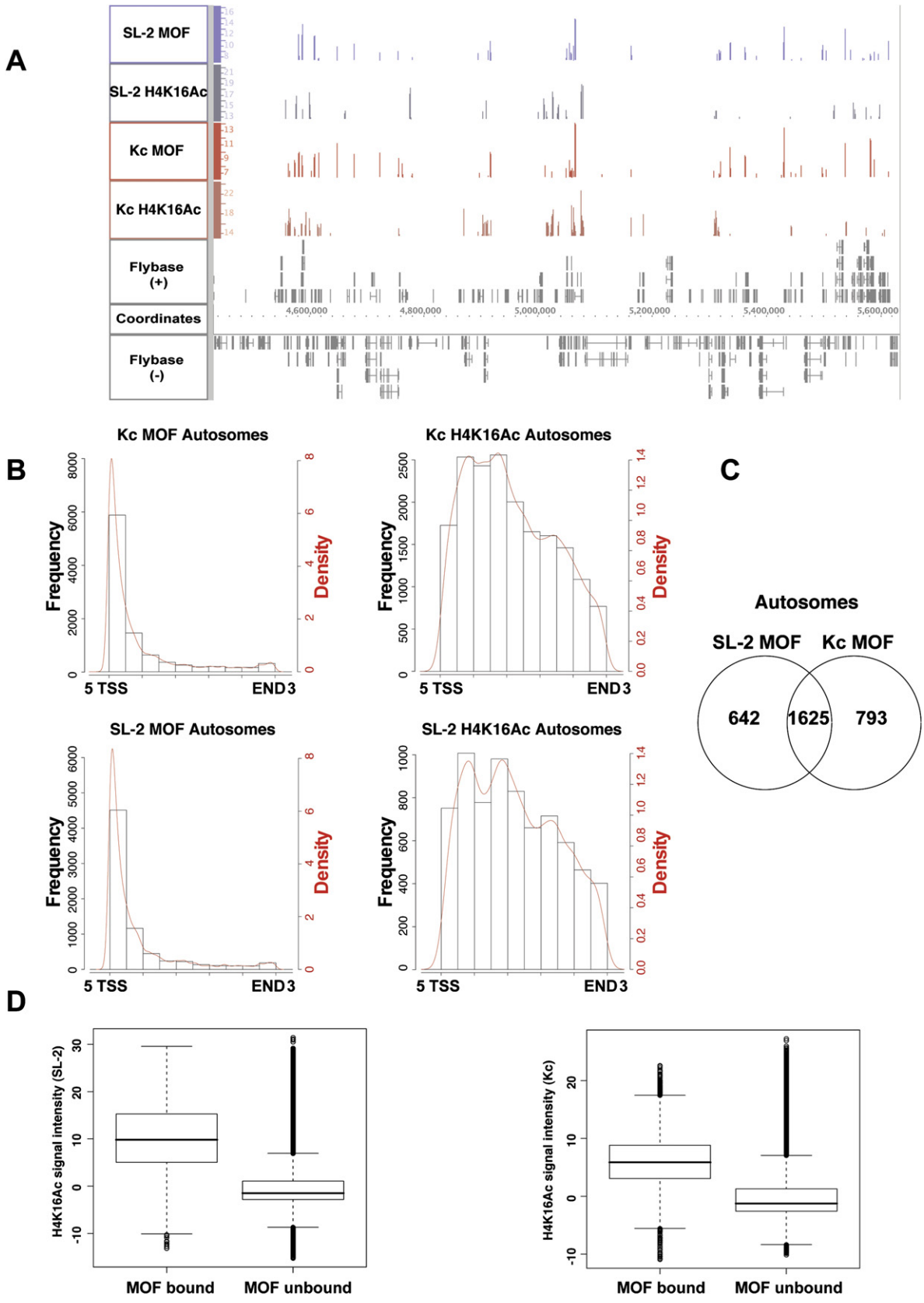
A
SL-2 MOF
SL-2 H4K16Ac
Kc MOF
Kc H4K16Ac
Flybase (+)
Coordinates
Flybase (-)
4,600,000
4,800,000
5,000,000
5,200,000
5,400,000
5,600,000
B
Kc MOF Autosomes
Kc H4K16Ac Autosomes
SL-2 MOF Autosomes
SL-2 H4K16Ac Autosomes
Frequency
Density
5 TSS
END 3
C
Autosomes
SL-2 MOF
Kc MOF
642
1625
793
D
H4K16Ac signal intensity (SL-2)
H4K16Ac signal intensity (Kc)
MOF bound
MOF unbound

binding of MOF to promoters of X-linked genes between SL-2 and Kc cells (Figure 3B) argues for MSL-independent targeting of MOF to promoters on the X chromosome. To test this hypothesis, we performed RNAi-mediated depletion of MSL1 followed by ChIP-qRT-PCR analysis to study MOF recruitment. We analyzed the four X-linked genes *CG8173, par-6, Ucp4a*, and the previously identified "high-affinity site" *roX2,* where MSL1 recruitment has been shown to be MOF independent (Kelley et al., 1999; Park et al., 2002). PCR primers were designed to span the promoter (P1), middle (P2), and end (P3) of each gene (See Experimental Procedures). In MSL1-depleted cells, binding of MOF is severely compromised across the lengths of all four genes tested as compared to the control EGFP RNAi-treated cells, whereas MOF binding to promoter-proximal regions remained unaffected (Figures 4A–4D).

Consistent with the ChIP-chip analysis, MOF was found to bind promoters on the same set of genes in Kc cells, without any substantial enrichment toward the interior of X chromosomal genes, with the exception of modest binding to the *roX2* high-affinity site (Figure S15A). The presence of MSL1 could not be detected above threshold levels on any of the other X-chromosomal genes in Kc cells, in agreement with polytene chromosome stainings (data not shown). Similarly, MOF displayed sole promoter occupancy for an X-chromosomal gene (*CG12094*) and three autosomal genes (*hbs1, frazzled [fra], gprk2*) in SL-2 cells that were not found to be enriched by MSL1 or MSL3 (Figure S15B). We therefore conclude that MOF recruitment to promoters is MSL-independent on dosage-compensated genes in both SL-2 and Kc cells, whereas MOF binding to the 3′ ends of these genes requires MSL1.

We have previously shown that sequences toward the 3′ end of two dosage-compensated genes contain targeting cues for the MSL complex (Kind and Akhtar, 2007). We were therefore interested in testing whether MSL1 and MSL3 target the 3′ end of genes independently of MOF, and whether MOF localization to the gene interior is MSL dependent. In agreement with previous studies on polytene chromosomes, MSL1 binding to *roX2* is only mildly affected upon MOF depletion. Since *roX2* is a high-affinity site where partial complexes containing MSL1 can assemble independently of MOF and MSL3, this experiment showed consistency with previously published data (Kelley et al., 1999; Park et al., 2002) and confirmed the reproducibility between both experiments (Figure 4H). However, MSL1 binding to the three dosage-compensated genes or low-affinity sites (*Ucp4A, par-6, CG8173*) is significantly reduced in cells depleted of MOF when compared to the EGFP RNAi control samples (Figures 4E–4G). Therefore, we conclude that MOF is essential for targeting of the MSL complex to dosage-compensated genes or low-affinity binding sites. In contrast, binding of MSL1 to high-affinity sites such as *roX2* is independent of MOF.

MOF Is Responsible for Bulk H4K16 Acetylation

Although MOF alone displays HAT activity in vitro (Akhtar and Becker, 2000), this has been shown to be enhanced when MOF is in complex with MSL1 and MSL3 (Morales et al., 2004). The shift in H4K16Ac 3′ enrichment on the X chromosome (Figure 2D) to 5′ enrichment on autosomes in SL-2 and Kc cells (Figure 3B), together with the correlation between MOF binding and H4K16Ac in both SL-2 and Kc cells (Figure 3D), suggests that MOF is active as a HAT on promoters independently of the MSL complex in vivo.

In order to test for HAT activity of MOF on promoters, we analyzed H4K16Ac levels for a subset of X-chromosomal (*CG8173, par-6, Ucp4A, roX2*) and autosomal (*hbs1, fra, gprk2*) genes by ChIP-qRT-PCR analysis in cells depleted of MOF (Figure 5). EGFP dsRNA-treated cells were used as controls. Control ChIP for histone H4 levels was performed in parallel for each condition. We were also eager to test whether the presence of MOF at promoters of X-chromosomal genes in the absence of MSL1 is sufficient for HAT activity. As shown in Figure 5, while histone H4 levels remain unaffected (gray plots), we observe that H4K16Ac on the target genes is markedly reduced upon MOF depletion on both X-chromosomal and autosomal targets compared to EGFP dsRNA-treated control cells (red plots). H4K16Ac levels in MSL1-depleted cells were reduced only on X-chromosomal genes, whereas in the case of autosomal MOF targets, H4K16Ac levels remained unaffected or showed only a slight increase. This could be due to an excess of available MOF protein following its apparent dissociation from the X chromosome (black plots). These results strongly suggest that MOF is directly involved in H4K16 acetylation of its target genes and that, in addition, MOF's activity on the X chromosome is coordinated by the other MSLs similar to the behavior observed in vitro (Morales et al., 2004).

These observations were further confirmed by mass spectrometric analysis of endogenous histones isolated from control EGFP- or MOF dsRNA-depleted SL-2 and Kc cells (Figure 6). MOF levels were depleted to approximately 20% of those observed in EGFP dsRNA-treated samples in SL-2 and Kc cells (Figure 6A). Interestingly, we found that at steady state only about 20% of histones were monoacetylated in SL-2 cells and approximately 15% in Kc cells. Of this monoacteylation, H4K16Ac was accounted for by approximately 29% and 23% of total acetylation in SL-2 and Kc cells, respectively. Depletion of MOF resulted in a clear reduction of lysine 16 acetylation, such that overall monoacetylation levels dropped to approximately 11% in both cell lines. In contrast, monoacetylation at H4K5 remained unaffected (Figure 6). Taken together, these

Figure 3. MOF Is Bound to Promoter-Proximal Regions on Autosomes in SL-2 and Kc Cells

(A) Binding profile of MOF and H4K16Ac in SL-2 and Kc cells on about 1 Megabase (MB) region of chromosome 2L. Flybase (+) and (−) represents the location of genes on the forward and reverse DNA strands, respectively. Coordinates represent the position on the corresponding chromosome.

(B) Probe frequency and density measurements of MOF binding and H4K16Ac to gene loci on the autosomes in SL-2 and Kc cells. Default binding of MOF to promoters in SL-2 and Kc cells results in a shift in the H4K16Ac pattern toward the 5′ end across gene loci.

(C) Overlap in MOF target genes between SL-2 and Kc cells on autosomes.

(D) MOF binding significantly correlates with H4K16Ac in both SL-2 ($p < 2e\text{-}16$) and Kc cells ($p < 2e\text{-}16$).

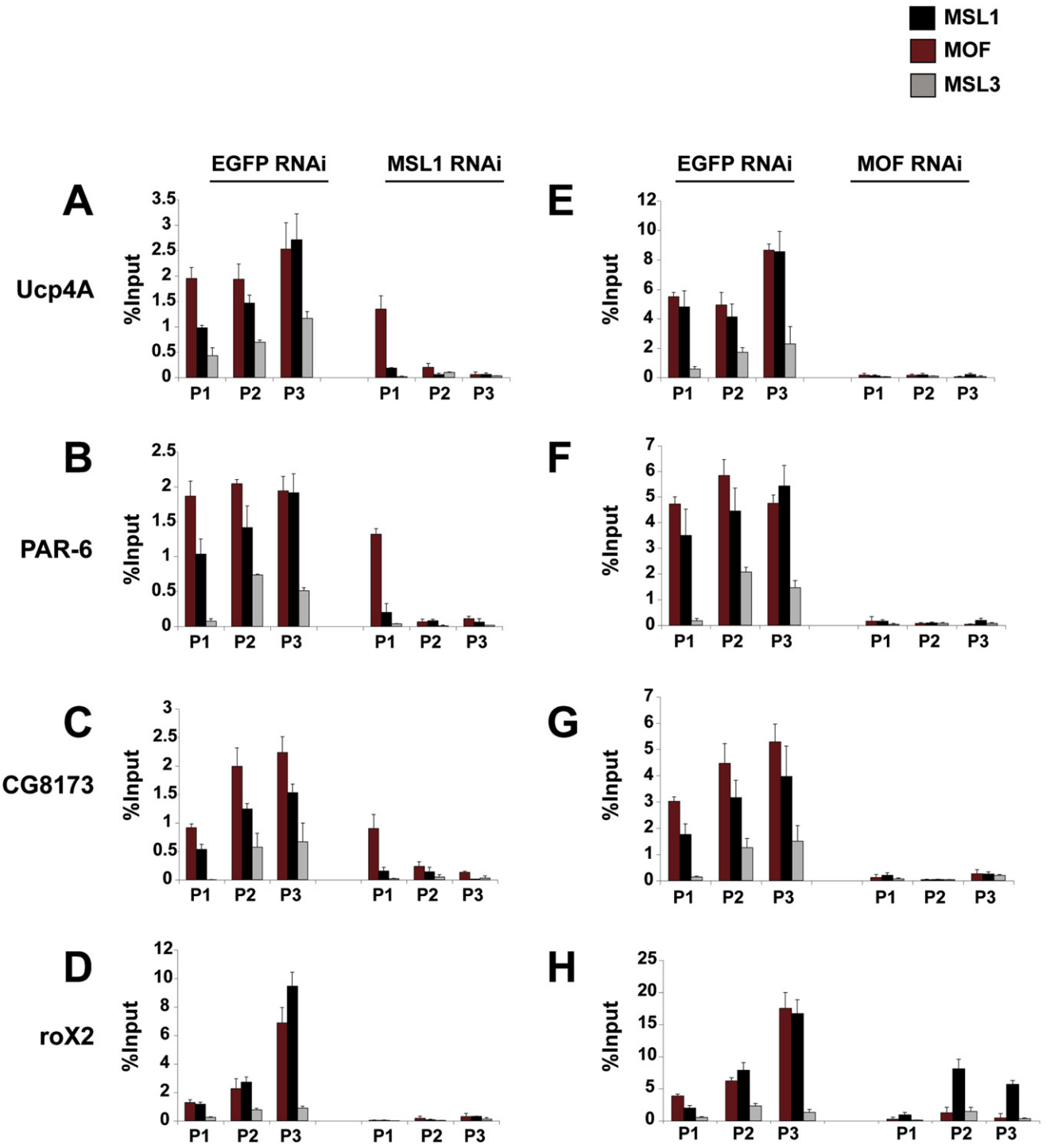

Figure 4. Binding of MOF to Promoters Is Independent of MSL1

(A–H) MOF is essential for targeting of MSL1 and MSL3 to X-linked genes, but does not itself require MSL1 for binding to promoters. Chromatin immunoprecipitation (ChIP) using MSL1 (black), MOF (red), and MSL3 (gray) antibodies in MSL1 (A–D) or MOF-depleted (E–H) cells. Binding of MSL1 (black), MOF (red), and MSL3 (gray) to the X-linked genes *ucp4a*, *par-6*, *CG8173*, *rox2* is shown. EGFP dsRNA-treated cells were used as controls. ChIP is shown as percentage recovery of input DNA. Primers were positioned at the promoter (P1), middle (P2), and end (P3) of genes. The exact position of the primers is described in the Supplemental Data. ChIP is shown as percentage recovery of input DNA (% Input). Error bars represent standard deviation (StDev) of three independent experiments.

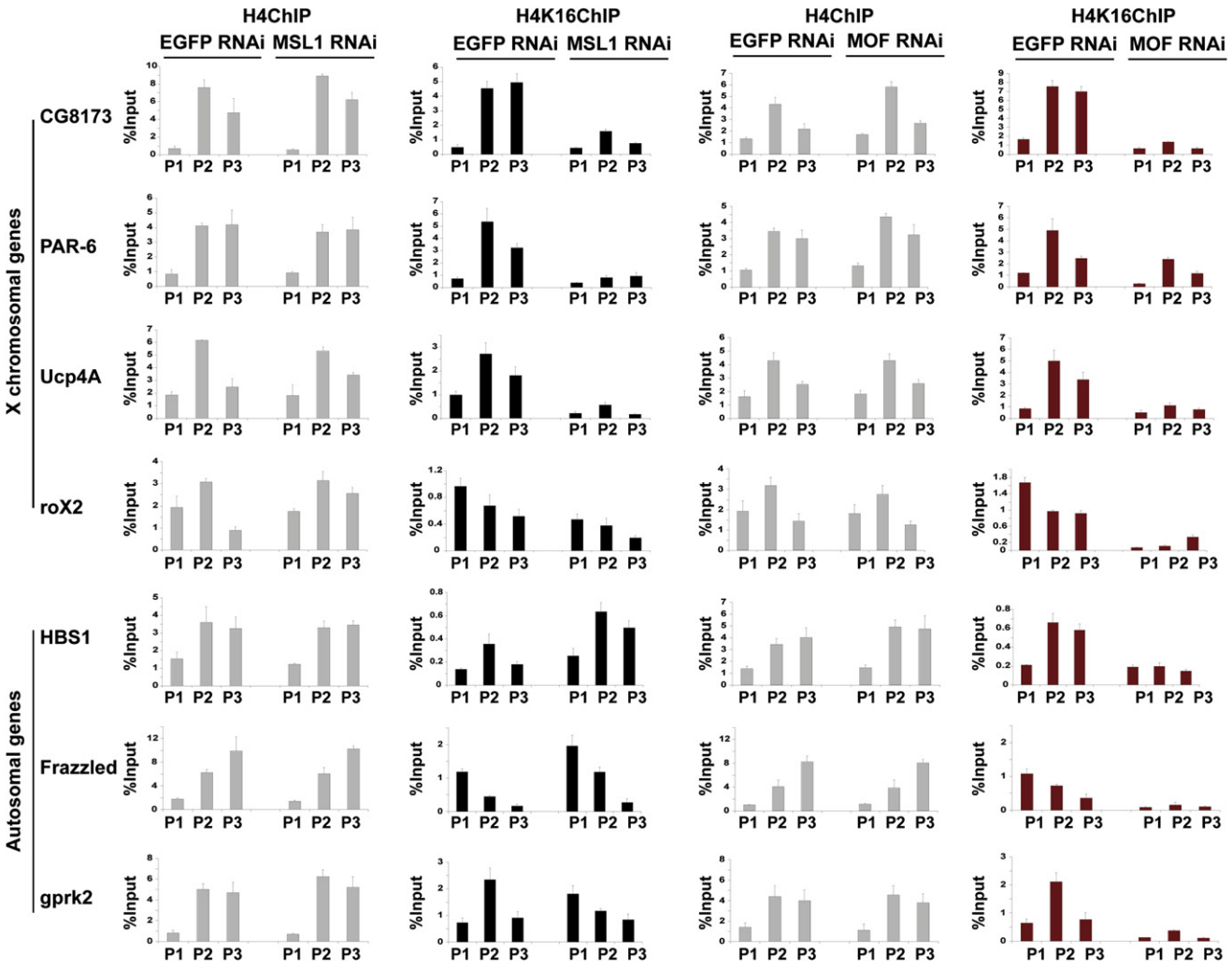

Figure 5. MOF Is Active as a Histone Acetyltransferase on Both the X Chromosome and Autosomes

Chromatin immunoprecipitation (ChIP) using histone H4 and H4K16Ac-specific antibodies on four X-linked genes *ucp4a*, *par-6*, *CG8173*, *roX2,* and three autosomal genes *hbs1, fra*, and *gprk2* in MSL1- (black) and MOF-depleted (red) cells. Histone H4 ChIP (gray) remained mostly unaffected in both MSL1 and MOF dsRNA-treated cells. Primers were positioned at the promoter (P1), middle (P2), and end (P3) of genes. Exact position of the primers is described in the Supplemental Data. ChIP is shown as percentage recovery of input DNA (% input). Error bars represent standard deviation (StDev) of three independent experiments.

results show that MOF is responsible for the bulk of H4K16 acetylation events in both SL-2 and Kc cells.

Dosage Compensation Acts Mainly by Local Binding of MSL Complexes

The correlation between MOF association and H4K16Ac in both SL-2 and Kc cells (Figures 3D and 5) prompted us to test for the transcriptional regulation of genes by MOF in both cell types by RNAi-mediated depletion followed by hybridization of the labeled transcript population to Affymetrix *Drosophila* 2 gene expression arrays (see Experimental Procedures). In addition, we also determined the expression profiles of SL-2 cells depleted of MSL1 and MSL3, in order to compare between regulation by MOF inside and outside the MSL context. All experiments were performed in triplicate and normalized against control EGFP dsRNA-treated samples. The three MSL proteins could be successfully depleted to a level between 10%–20% compared to EGFP RNAi-treated cells (Figure S16).

Overall, MOF depletion resulted in the most significant number of differentially expressed genes, followed by MSL3 and MSL1 in SL-2 cells (Figures 7A–7D). MSL1 depletion results in downregulation of primarily X-chromosomal genes. On the X chromosome, almost all affected genes were found to be downregulated (Figure 7D). Interestingly, where an MSL1 knockdown almost exclusively affects X-chromosomal genes, MSL3 and MOF RNAi treatment results in both up- and downregulation of autosomal genes (Figures 7A–7D). Genes affected by MOF and MSL3 could be subcategorized into various biological functions with certain emphasis on cell cycle-related processes (Table S4). We next tested whether genes that were only upregulated (252 genes) or downregulated (217 genes) by MSL3 on autosomes were associated with a particular biological process. However, our

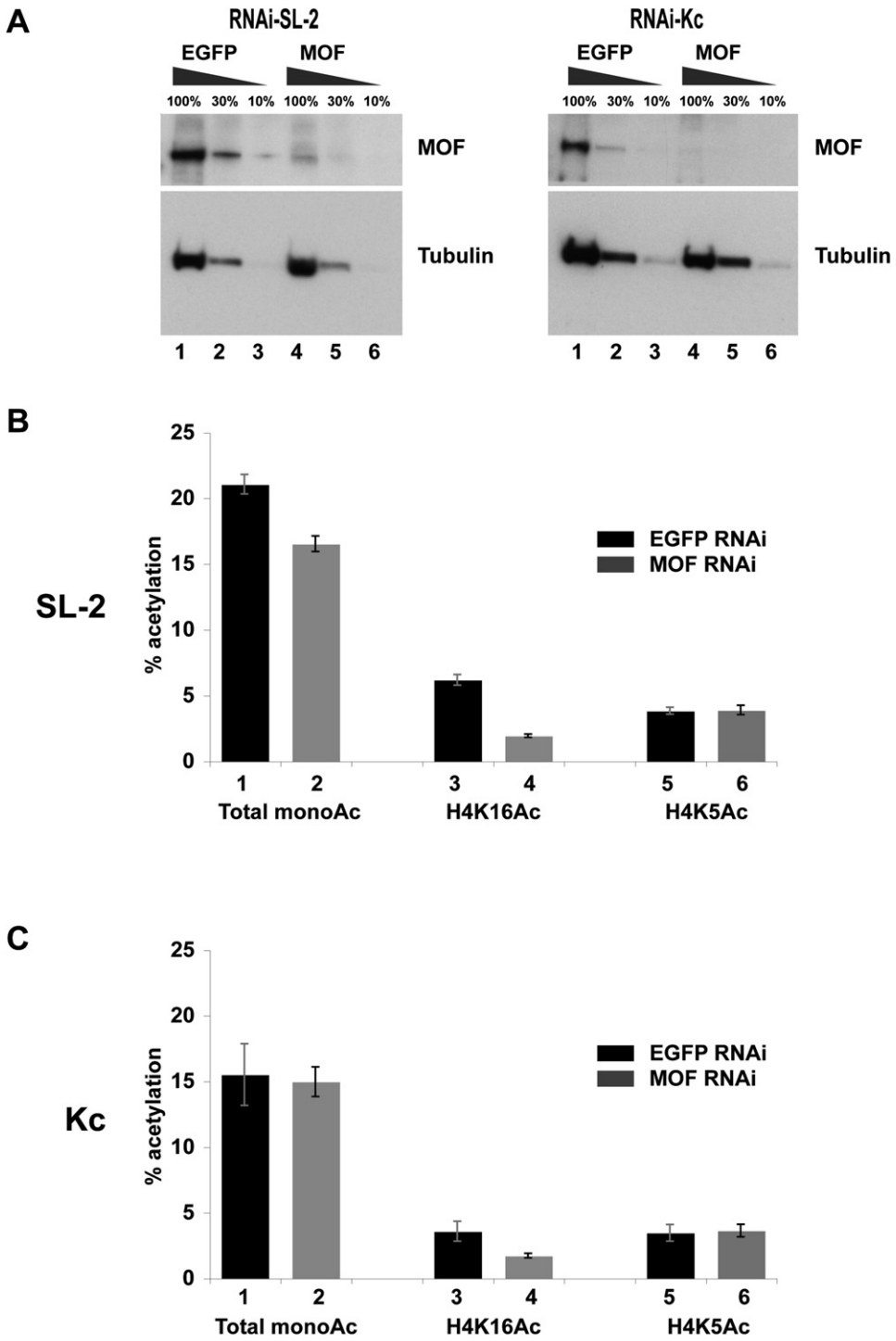

Figure 6. Global Levels of H4K16Ac Are Affected upon MOF Depletion in Both SL-2 and Kc Cells

(A–C) Relative quantitative analysis of acetylation of histone H4 sites K5/K8/K12 and K16 by mass spectrometry. (A) shows western blot analysis of the efficiency of MOF depletion in SL-2 (right panel) and Kc cells (left panel). Dilution of the corresponding extracts is indicated. (B) shows Monoacetylated peptides containing the four acetylation sites (amino acid [aa] 4–17) in relation to nonacetylated peptide H4 in SL-2 (B) and Kc (C) cells. Columns 1 and 2, total amount of monoacetylated peptide as fraction of nonacetylated peptide population; Columns 3 and 4, K16-monoacetylated peptide as of fraction nonacetylated peptide population; columns 5 and 6, K5-monoacetylated nonacetylated peptide population. MOF-directed dsRNA interference (MOF RNAi, gray columns) in SL-2 cells leads to a reduction of the total fraction of monoacetylated peptide in comparison with an unrelated (EGFP RNAi, black columns) control. Site-specific analysis reveals that H4K16 acetylation reflects loss of acetylation, while K5 acetylation remains unaffected. In contrast, in Kc cells overall monoacetylation seems to be only slightly affected by dsRNA interference. Nevertheless, H4K16 site-specific monoacetylation is reduced by a factor of 2, indicating a significant contribution to

analysis did not reveal a particularly intriguing overrepresented category (Tables S5 and S6).

The majority of genes downregulated on the X chromosome are bound by MSL1, MSL3, or MOF (Figure 7E). We confirmed this finding by ChIP with MOF and MSL1, followed by qRT-PCR analysis of SL-2 cells depleted of these proteins for 18 genes in an approximately 150 kb region (see Figure S4). As shown in Figure 7E, genes bound by MSL1 and MOF generally show good correlation with differentially downregulated genes in the cells depleted for MOF and MSL1 (compare upper and lower panels of Figure 7F). The minority of genes that are differentially expressed but not bound could be either secondary targets or genes distally regulated via long-range elements. We conclude that, in general, genes on the X chromosome that are subject to dosage compensation are directly bound by the MSL complex in agreement with previous studies (Alekseyenko et al., 2006; Gilfillan et al., 2006).

On autosomes, approximately 30% of the genes differentially regulated in MOF-deprived cells are bound (Figure S17). In Kc cells, we observed that a similar number of downregulated genes were bound by MOF but only 15% of the upregulated genes comprise real targets (Figure S17). We verified gene regulation by MOF of three target genes (*hbs1, fra, gprk2*) shown to display reduced H4K16Ac levels upon MOF depletion (Figure 5). We could confirm that for all three genes expression levels were reduced approximately 2-fold (Figure S18). Interestingly, although MSL1 depletion showed no effect on *hbs1* and *fra*, expression of *gprk2* was reduced similar to a MOF knockdown, indicating that in exceptional cases MSL1 is involved in the regulation of some genes on the autosomes. Taken together, these findings further support a role for MOF in the regulation of expression of genes on the X chromosome and a subset of autosomal genes.

DISCUSSION

Differential Distribution of the MSL Complex Members on Target Genes

Consistent with previous MSL1 and MSL3 profiling studies (Alekseyenko et al., 2006; Gilfillan et al., 2006; Legube et al., 2006), we show that MSL1, MSL3, MOF, and H4K16Ac display enrichment to 3′ end of genes in SL-2 cells. Surprisingly, MOF displays a bimodal binding pattern on genes residing on the X chromosome, associating with both the 3′ ends of dosage-compensated genes as well as with promoter regions.

Our recent observations on individual X-chromosomal target genes using transgene analysis in vivo have revealed that there are at least two classes of sites; transcription-independent ''high-affinity sites'' such as *roX2* and transcription-dependent ''low-affinity sites'' such as *mof* or *CG3016* (Kind and Akhtar, 2007). Integrating the observations obtained from the genome-wide binding and RNAi-mediated knockdown analysis shown here, it appears that MOF plays a central role in targeting the MSL complex to ''low-affinity sites'' where recruitment of MSL1 and MSL3 is found to be dependent on the presence of MOF. This is in contrast to the ''high-affinity sites'' where partial complexes of MSL1/MSL2 can be recruited independently of MOF, MSL3, and MLE (Dahlsveen et al., 2006).

Interestingly, we found that MOF binds not only to the male X chromosome, but also to autosomes and female chromosomes (Figure S3). Different from the bimodal binding pattern of MOF on the male X chromosome, in Kc cells, MOF is enriched to promoters of all chromosomes similarly to the situation on the male autosomes in SL-2 cells (Figures 3B and S10). However, although the binding pattern between the X and the autosomes in Kc cells looks practically identical, the amplitude of promoter binding is significantly higher on the X chromosome than on the autosomes in Kc cells, as is the case in SL-2 cells (Figure S13). It is possible that X-chromosomal genes have as-yet-unidentified sequence elements that contribute toward MOF binding to promoters of X-chromosomal genes in males and females. Alternatively, since reduced amount of MSL1 is expressed in females (Kelley et al., 1995) and MSL1 displays low-level promoter binding on the X chromosome in SL-2 cells, it may contribute to higher amplitude of MOF binding on X chromosomal genes in both SL-2 and Kc cells compared to autosomes (Figures 2A, 2E, and S8). As the gene density on the X chromosome is similar to that of other chromosomes (except for the fourth chromosome), this does not explain the higher amplitude of MOF binding on the X chromosome. It is therefore possible that MOF, in addition to its role in facilitating transcriptional elongation by acetylating gene loci in an MSL context, is also involved in transcriptional initiation in an MSL-independent manner, perhaps by interaction with additional factors. Another interesting possibility is that the enrichment of MOF to promoters may provide a reservoir of enzyme, held in check by other factors, to be readily used by the MSL proteins or other promoter-bound complexes when needed for modulating transcription levels.

Intriguingly, the MSL3 profile across gene loci appeared very similar to that of H4K16Ac (Figures 2A–2D), suggesting a role for MSL3 in activation and/or stabilization of H4K16Ac on X-linked genes. In support of this hypothesis, MSL3 has been shown to stimulate MOF's HAT activity in vitro (Morales et al., 2004). Recently, MSL3 was shown to bind H3K36 trimethylated (H3K36me3) nucleosomes, and H3K36me3 (which also peaks at 3′ end of genes, similar to MSLs) was shown to influence MSL binding (Bell et al., 2008; Larschan et al., 2007). In *S. cerevisiae*, Eaf3 recognition of H3K36me3 has been shown to direct Rpd3(S) to actively transcribed genes to deacetylate histones in the wake of polymerase II, preventing spurious transcription within genes from cryptic promoters (Carrozza et al., 2005). It has been proposed that the MSL complex on the X chromosome may compete for the Rpd3(S) complex, thereby increasing the overall H4K16Ac levels by reducing the turnover rates of this modification (Larschan et al., 2007).

As the 3′ ends of genes are indispensable for MSL target recognition on the X chromosome (Kind and Akhtar, 2007), we propose that MSL1 and MSL2 initially target 3′ regions by occasional recognition of degenerative DNA target elements

H4K16 acetylation by MOF-dependent activity in Kc cells. Error bars represent standard error of mean (SEM) of at least three independent experiments. See also Supplemental Experimental Procedures.

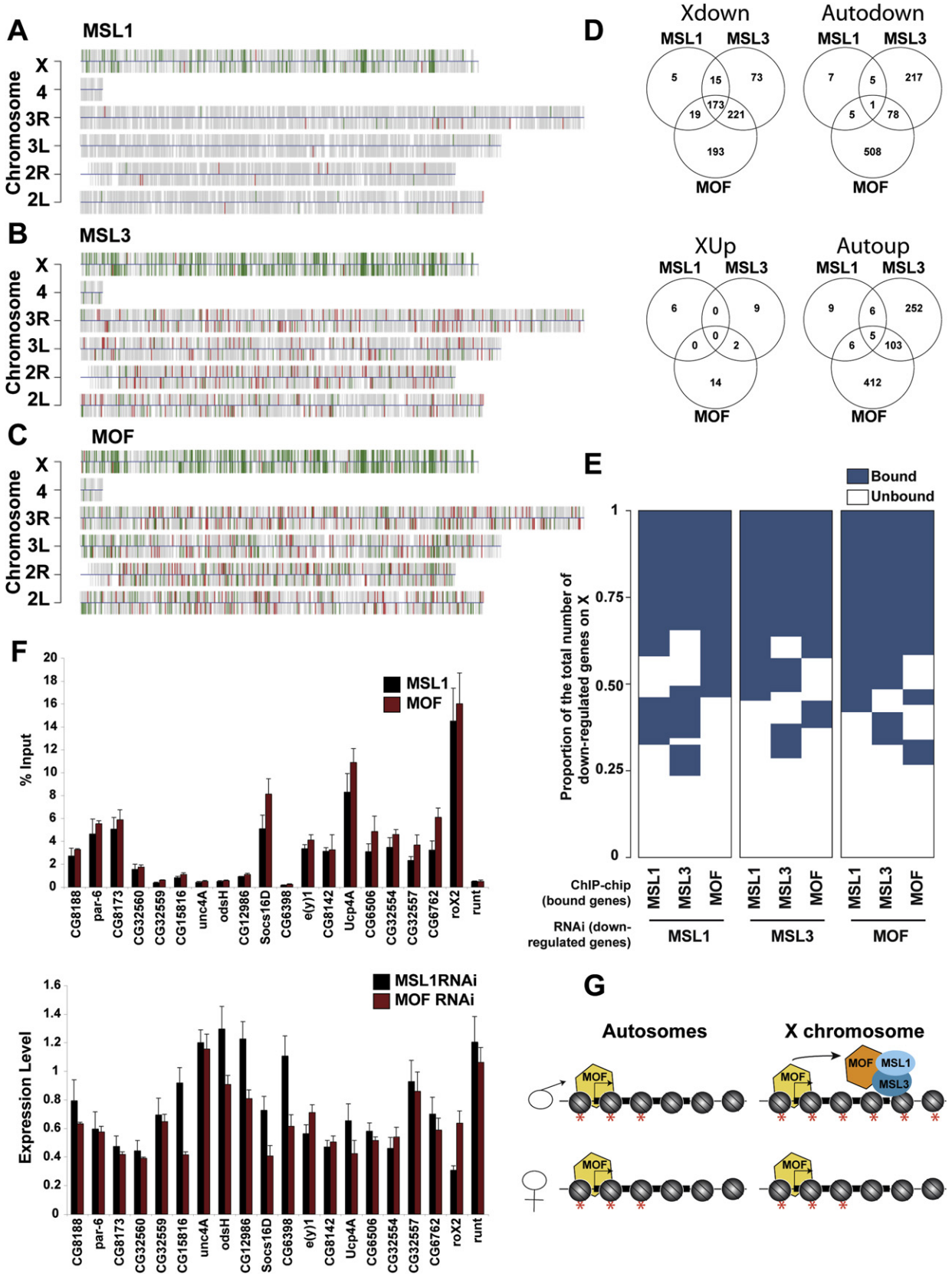
A
MSL1
B
MSL3
C
MOF
Chromosome
X
4
3R
3L
2R
2L
D
Xdown
Autodown
XUp
Autoup
MSL1
MSL3
MOF
5
15
73
19
173
221
193
7
5
217
5
1
78
508
6
0
9
0
0
2
14
9
6
252
6
5
103
412
E
Bound
Unbound
Proportion of the total number of down-regulated genes on X
1
0.75
0.50
0.25
0
ChIP-chip (bound genes)
RNAi (down-regulated genes)
F
% Input
MSL1
MOF
CG8188
par-6
CG8173
CG32560
CG32559
CG15816
unc4A
odsH
CG12986
Socs16D
CG6398
e(y)1
CG8142
Ucp4A
CG6506
CG32554
CG32557
CG6762
roX2
runt
MSL1RNAi
MOF RNAi
Expression Level
G
Autosomes
X chromosome

(Dahlsveen et al., 2006; Gilfillan et al., 2006; Kind and Akhtar, 2007), possibly made accessible by low levels of H4K16Ac brought about by MOF occupancy of the promoter. MSL3 may serve to stabilize the association of MSL1/MSL2 with dosage-compensated genes by binding to H3K36me3, which in turn may lead to the recruitment and stimulation of MOF to the body of the gene. It has also been proposed that local recycling of RNA polymerase II could result in enhanced mRNA production (Schubeler, 2006; Smith et al., 2001). MOF, with its enrichment to promoter-proximal and 3′ regions, is a likely candidate to bridge such a loop formation. Gene structural studies should reveal whether such a gene-loop formation is involved in the process of dosage compensation.

MOF, H4K16 Acetylation, and Gene Regulation

Here we present four independent lines of evidence that show that MOF is involved in H4K16Ac of a large number of genes in the male and female genome. A: MOF binding significantly correlates with H4K16Ac of all chromosomes in both SL-2 and Kc cells (Figure 3D). B: The H4K16Ac profile across genes correlates strongly with the diversified binding of MOF between the X chromosome (peaking toward the 3′ end of genes), and autosomes (peaking toward the 5′ end of genes [compare Figures 2C–2D with 3B]). C: Depletion of MOF results in a marked decrease in H4K16Ac of a number of genes on both the X chromosome and the autosomes (Figure 5). D: In MOF-depleted SL-2 and Kc cells we find a more than 50% reduction in total H4K16Ac levels by mass specterometery analysis (Figure 6).

Several studies have implied a structural role for histone acetylation and H4K16Ac acetylation in particular, in the packaging of DNA into chromatin. Interestingly, H4K16Ac has been shown to cause an increase in the α-helical content of histone H4, and to prevent 30 nm chromatin-fiber formation and crossfiber interactions (Shogren-Knaak et al., 2006). H4K16Ac might therefore serve a structural role, imparting a relaxed chromatin state that, in turn, reduces the energy required for RNA polymerase II to affect transcription through a nucleosomal template and thereby enhancing elongation efficiency (Calestagne-Morelli and Ausio, 2006).

Regulation of ubiquitously expressed (housekeeping) genes on the X chromosome by the MSL complex (Legube et al., 2006; Gilfillan et al., 2006) probably necessitates a state of continual association with its target binding sites. Elevated levels of H4K16Ac are reached on the X chromosome presumably by constant activation of MOF by MSL1 and MSL3. On the autosomes, since MOF appears to be present independently of other MSL proteins, it does not associate to the interior of gene loci but is instead promoter bound, similar to its behavior on the X chromosome in the MSL1-depleted condition (Figure 4).

Assuming that MOF is involved in general transcription regulation, apart from dosage compensation, it is not surprising that MOF is required for most H4K16 acetylation (Figure 6). Similarly, MOF in mammals has been found to be responsible for most, if not all, H4K16Ac (Smith et al., 2005; Taipale et al., 2005). Interestingly, in line with a possible role for MOF in the G2/M cell-cycle checkpoint in mammals (Taipale et al., 2005) we found that in both SL-2 and Kc cells, MOF-bound targets are significantly enriched for certain cell-cycle functional categories (Tables S1, S2, and S3). It would therefore be very interesting to study gene regulation by MOF in a cell-cycle context in synchronized cells.

The role of MOF mediated H4K16Ac on the autosomes remains speculative. H4K16Ac modification on autosomes by MOF may create an opportunity for transcription initiation/reinitiation, rather than being an essential mark for transcriptional activity itself (Anguita et al., 2001). This could also explain why we observe that, although MOF is generally bound to active genes (Figure S14), approximately 30% of the autosomal bound genes are affected by MOF depletion (Figure S17). MOF's presence on autosomal genes may therefore provide a minimal landscape of H4K16Ac, maintaining a local environment with relatively open chromatin structure, presumably similar to the condition of mating type loci in yeast (Johnson et al., 1990; Megee et al., 1990). Upon transcriptional cues, those genes would be able to rapidly and efficiently respond to meet the cell's requirements, as would be the case for cell cycle-related genes (as discussed above).

Second, MOF may work together with as-yet-uncharacterized proteins, which may allow RNA polymerase II to move efficiently through the chromatin template similar to the situation on the X chromosome. In fully elucidating the molecular mechanisms behind this process, a vital step will be the characterization of additional protein complexes associated with MOF, apart from

Figure 7. Dosage Compensation Acts by Upregulation of the X Chromosome on a Gene-by-Gene Basis

(A–C) Genome distribution of differentially expressed genes in MSL1-, MSL3-, and MOF-depleted SL-2 cells. Downregulated genes (green lines) and upregulated genes (red lines) are shown. The white areas on the chromosomes indicate the position of genes.

(D) Venn diagram representing overlap of up- or downregulated genes on the X chromosome or autosomes.

(E) Correlation between differential expression and MSL1, MSL3, and MOF binding on the X chromosome in SL-2 cells. Each major column represents genes significantly downregulated in the MSL1, MSL3, and MOF RNAi depletion assays, respectively (note that each group of columns represent different numbers of genes, as shown in D). Within each group, the proportion of genes bound by MSL1, MSL3, and MOF in the ChIP-chip experiments is shaded in blue (minor columns). Genes were sorted by hierarchical clustering within each group. Unbound genes are represented as white sections. y axis represents the proportion of the total number of downregulated genes on the X chromosome.

(F) Correlation between binding (top) and expression (bottom) of 18 genes on the X chromosome by qRT-PCR. MOF is depicted in red and MSL1 is shown in black. Error bars represent standard deviation (StDev) of three independent experiments for both ChIP and expression analysis.

(G) Working model for MOF recruitment on X-linked and autosomal genes. Our data suggest that MOF is recruited to promoter-proximal regions independently of MSL1 and MSL3. In the context of the X chromosome, the concerted action of other complex members, such as MSL1 and MSL3, allows recruitment of MOF throughout gene loci, resulting in more extended acetylation over intragenic regions peaking toward the 3′ end. In contrast, on autosomes H4K16 acetylation marks are most abundant toward the 5′ ends of genes, directly reflecting the distribution of MOF binding sites. A broader distribution of MOF protein on X-linked genes, together with an extended H4K16 acetylation, may therefore confer efficient transcriptional elongation. While on autosomes, 5′-end acetylation may affect a poised state of transcriptional potential, facilitating more effective transcription factor binding and/or promoting transcription initiation. H4K16Ac is represented as red asterisks.

the MSL complex (Dou et al., 2005; Mendjan et al., 2006; Smith et al., 2005). We propose that such complexes, comprising different *trans*-activating or repressive factors, may modulate MOF's HAT activity resulting in differential transcriptional outputs. Furthermore, MOF binding to promoters may allow efficient and rapid response to cellular events by recruitment/exclusion of H4K16 binding proteins or, more generally, by unique H4K16Ac-induced conformational changes to the chromatin fiber. Interestingly, one of the evolutionary conserved interacting partners of MOF is WDS, a protein in mammals shown to associate with histone H3 lysine 4 methylation, a histone mark enriched at promoters (Dou et al., 2005; Han et al., 2006; Mendjan et al., 2006; Wysocka et al., 2005). It would be interesting to study the potential involvement of WDS or other promoter-bound factors in recruiting MOF to promoters.

In summary, this study has revealed that the MSL complex members do not conform to a uniform binding behavior on their target genes on the X chromosome, MSL1 and MSL3 are enriched at the 3′ end of genes, while MOF shows a bimodal distribution with enrichment at promoter-proximal regions as well as 3′ ends. Our data reveal that MOF plays a central role in the targeting process on low-affinity sites where recruitment of MSL1 and MSL3 appear to be dependent on the presence of MOF, in contrast to high-affinity sites such as *roX2* where targeting of MSL1 appears to be MOF independent. Furthermore, the previously unappreciated binding of MOF to promoter-proximal regions on X-chromosomal as well as autosomal sites provides an opportunity to investigate additional roles of this enzyme in other cellular processes.

EXPERIMENTAL PROCEDURES

Chromatin immunoprecipitation (ChIP)

All ChIP experiments were performed at least three times using independent chromatin preparations. The antibodies for MSL1, MSL3, and MOF are as described in Mendjan et al. (2006). Anti-H4K16Ac (ab23352) and anti-Histone H4 (ab10158) rabbit polyclonal antibodies are from Abcam. SL-2 cells were grown in Schneider medium (GIBCO) containing 10% FCS. 1×10^8 cells were cross-linked with formaldehyde for 8 min. Sonication was performed for 26 × 30 s at input 5 (Bioruptor, Diagenode) in lysis buffer (50 mM HEPES/KOH at pH 7.5, 500 mM NaCl, 1 mM EDTA, 1% Triton X-100, 0.1% DOC, 0.1% SDS + Complete protease inhibitors [Roche]). One hundred micrograms of chromatin and three microliters of polyclonal antibody was used per IP. Immunocomplexes were isolated by adding protein A/G-Sepharose (Roche) followed by four washing steps: 2x lysis buffer, 1x DOC buffer (10 mM Tris at pH 8, 0.25 M LiCl, 0.5% NP-40, 0.5% DOC, 1 mM EDTA), and 1x TE at pH 8. DNA was eluted in 1X elution buffer (1% SDS, 0.1 M NaHCO3) for 20 min RT followed by reversal of crosslinks at 65°C O/N. DNA was purified by a 30 min incubation at 37°C RNaseA (0.2 mg/ml), followed by 2 hr Proteinase K digestion (0.05 mg/ml), phenol/chlororform exctraction, and DNA precipitation. ChIP DNA samples were resuspended in 100 μl TE. We used 1 μl ChIP material for each Q-PCR reaction.

Processing and Hybridization of ChIP DNA

Processing of the ChIP DNA samples for hybridization was performed according to Legube et al. (2006). Hybridization, washing, and scanning of arrays followed the Affymetrix ChIP-chip protocols.

ChIP-Chip and Expression Data Analyses and Availability

Details on ChIP-chip and gene expression data analyses are available as Supplemental Experimental Procedures.

RNA Interference (RNAi)

RNAi of SL-2 and Kc cells was performed as described in (Worby et al., 2001) with the following modifications. All knockdowns cells were incubated with 45 μg dsRNA. The cells were harvested after 4 days for MSL1 RNAi and 7 days for MSL3 and MOF RNAi. For both time points, GFP control RNAi experiments were performed in parallel.

Quantitative Real-Time PCR

qRT-PCR analysis of the ChIP samples was performed using the SYBR Green PCR master mix (Applied Biosystem), 100 ng of each forward and reverse primer, and 1 μl immunoprecipitated DNA, in an ABI7500 real-time PCR thermocycler (Applied Biosystems, Inc.). The formula [% ChIP/input] = $[E^{(Ct_{input} - Ct_{ChIP})} * 100\%]$ (where E represents primer annealing efficiency) was used to calculate the percentage DNA recovery after ChIP as compared to the amount of input material. For quantitation of transcript levels, RNA was first reverse transcribed using the SuperScript RT (Invitrogen), and 500 ng random hexamers. One microliter of cDNA was then subjected to real-time PCR using the SYBR Green PCR master mix (Applied Biosystems) and 100 ng of each primer. The primers designed in the middle of the genes in the ChIP experiment were used for the analysis of the transcript levels.

Immunostaining of Polytene Chromosomes

Preparation of polytene chromosomes was performed as described (http://www.igh.cnrs.fr/equip/cavalli/Lab%20Protocols/Immunostaining.pdf). Rat MSL3 and rabbit MOF antibodies were used at 1:500 dilution. Images were captured with an AxioCamHR CCD camera on a Zeiss Axiovert 200 M microscope using a 100x PlanApochomat NA 1.4 oil immersion objective.

ACCESSION NUMBERS

Microarray data are available in the ArrayExpress database (Parkinson et al., 2007) under accession numbers E-MEXP-1508 (ChIP-chip records) and E-MEXP-1505 (gene expression records).

SUPPLEMENTAL DATA

Supplemental Data include 18 figures, 6 tables, Supplemental Experimental Procedures, and Supplemental References and can be found with this article online at http://www.cell.com/cgi/content/full/133/5/813/DC1/.

ACKNOWLEDGMENTS

We are grateful to Jos de Graaf, Tomi Bähr-Ivacevic, and Vladimir Benes (EMBL Genomic Core Facility) for sample processing and hybridization to the Affymetrix tiling and expression arrays. We are also grateful to the members of the Akhtar lab and to Wolfgang Huber and Richard Bourgon for helpful suggestions, and to Lars Steinmetz and François Spitz for critical reading of the manuscript. This work was supported by SPP1129 (Epigenetics) and Epigenome NoE under the EU Framework Programme 6 to A.A. P.G. is supported by an "E-STAR" fellowship funded by the EC's FP6 Marie Curie Host fellowship for Early Stage Research Training under contract number MEST-CT-2004-504640.

Received: December 9, 2007
Revised: March 10, 2008
Accepted: April 29, 2008
Published: May 29, 2008

REFERENCES

Akhtar, A., and Becker, P.B. (2000). Activation of transcription through histone H4 acetylation by MOF, an acetyl transferase essential for dosage compensation in Drosophila. Mol. Cell *5*, 367–375.

Alekseyenko, A.A., Larschan, E., Lai, W.R., Park, P.J., and Kuroda, M.I. (2006). High-resolution ChIP-chip analysis reveals that the Drosophila MSL complex selectively identifies active genes on the male X chromosome. Genes Dev. *20*, 848–857.

Anguita, E., Johnson, C.A., Wood, W.G., Turner, B.M., and Higgs, D.R. (2001). Identification of a conserved erythroid specific domain of histone acetylation across the alpha-globin gene cluster. Proc. Natl. Acad. Sci. USA *98*, 12114–12119.

Bashaw, G.J., and Baker, B.S. (1995). The msl-2 dosage compensation gene of Drosophila encodes a putative DNA- binding protein whose expression is sex specifically regulated by Sex- lethal. Development *121*, 3245–3258.

Bell, O., Conrad, T., Kind, J., Wirbelauer, C., Akhtar, A., and Schubeler, D. (2008). Transcription-coupled methylation of histone H3 at lysine 36 regulates dosage compensation by enhancing recruitment of the MSL complex in Drosophila. Mol. Cell. Biol. *28*, 3401–3409.

Bhadra, U., Pal-Bhadra, M., and Birchler, J.A. (1999). Role of the male specific lethal (msl) genes in modifying the effects of sex chromosomal dosage in Drosophila. Genetics *152*, 249–268.

Bone, J.R., Lavender, J., Richman, R., Palmer, M.J., Turner, B.M., and Kuroda, M.I. (1994). Acetylated histone H4 on the male X chromosome is associated with dosage compensation in Drosophila. Genes Dev. *8*, 96–104.

Calestagne-Morelli, A., and Ausio, J. (2006). Long-range histone acetylation: biological significance, structural implications, and mechanisms. Biochem. Cell Biol. *84*, 518–527.

Carrozza, M.J., Li, B., Florens, L., Suganuma, T., Swanson, S.K., Lee, K.K., Shia, W.J., Anderson, S., Yates, J., Washburn, M.P., and Workman, J.L. (2005). Histone H3 methylation by Set2 directs deacetylation of coding regions by Rpd3S to suppress spurious intragenic transcription. Cell *123*, 581–592.

Corona, D.F., Clapier, C.R., Becker, P.B., and Tamkun, J.W. (2002). Modulation of ISWI function by site-specific histone acetylation. EMBO Rep. *3*, 242–247.

Dahlsveen, I.K., Gilfillan, G.D., Shelest, V.I., Lamm, R., and Becker, P.B. (2006). Targeting determinants of dosage compensation in Drosophila. PLoS Genet. *2*, e5.

Dion, M.F., Altschuler, S.J., Wu, L.F., and Rando, O.J. (2005). Genomic characterization reveals a simple histone H4 acetylation code. Proc. Natl. Acad. Sci. USA *102*, 5501–5506.

Dou, Y., Milne, T.A., Tackett, A.J., Smith, E.R., Fukuda, A., Wysocka, J., Allis, C.D., Chait, B.T., Hess, J.L., and Roeder, R.G. (2005). Physical association and coordinate function of the H3 K4 methyltransferase MLL1 and the H4 K16 acetyltransferase MOF. Cell *121*, 873–885.

Duncan, K., Grskovic, M., Strein, C., Beckmann, K., Niggeweg, R., Abaza, I., Gebauer, F., Wilm, M., and Hentze, M.W. (2006). Sex-lethal imparts a sex-specific function to UNR by recruiting it to the msl-2 mRNA 3′ UTR: translational repression for dosage compensation. Genes Dev. *20*, 368–379.

Gilfillan, G.D., Straub, T., de Wit, E., Greil, F., Lamm, R., van Steensel, B., and Becker, P.B. (2006). Chromosome-wide gene-specific targeting of the Drosophila dosage compensation complex. Genes Dev. *20*, 858–870.

Han, Z., Guo, L., Wang, H., Shen, Y., Deng, X.W., and Chai, J. (2006). Structural basis for the specific recognition of methylated histone H3 lysine 4 by the WD-40 protein WDR5. Mol. Cell *22*, 137–144.

Hilfiker, A., Hilfiker-Kleiner, D., Pannuti, A., and Lucchesi, J.C. (1997). mof, a putative acetyl transferase gene related to the Tip60 and MOZ human genes and to the SAS genes of yeast, is required for dosage compensation in Drosophila. EMBO J. *16*, 2054–2060.

Horak, C.E., and Snyder, M. (2002). ChIP-chip: a genomic approach for identifying transcription factor binding sites. Methods Enzymol. *350*, 469–483.

Johnson, L.M., Kayne, P.S., Kahn, E.S., and Grunstein, M. (1990). Genetic evidence for an interaction between SIR3 and histone H4 in the repression of the silent mating loci in Saccharomyces cerevisiae. Proc. Natl. Acad. Sci. USA *87*, 6286–6290.

Kelley, R.L., Solovyeva, I., Lyman, L.M., Richman, R., Solovyev, V., and Kuroda, M.I. (1995). Expression of msl-2 causes assembly of dosage compensation regulators on the X chromosomes and female lethality in Drosophila. Cell *81*, 867–877.

Kelley, R.L., Meller, V.H., Gordadze, P.R., Roman, G., Davis, R.L., and Kuroda, M.I. (1999). Epigenetic spreading of the Drosophila dosage compensation complex from roX RNA genes into flanking chromatin. Cell *98*, 513–522.

Kind, J., and Akhtar, A. (2007). Cotranscriptional recruitment of the dosage compensation complex to X-linked target genes. Genes Dev. *21*, 2030–2040.

Kurdistani, S.K., and Grunstein, M. (2003). Histone acetylation and deacetylation in yeast. Nat. Rev. Mol. Cell Biol. *4*, 276–284.

Kurdistani, S.K., Tavazoie, S., and Grunstein, M. (2004). Mapping global histone acetylation patterns to gene expression. Cell *117*, 721–733.

Larschan, E., Alekseyenko, A.A., Gortchakov, A.A., Peng, S., Li, B., Yang, P., Workman, J.L., Park, P.J., and Kuroda, M.I. (2007). MSL complex is attracted to genes marked by H3K36 trimethylation using a sequence-independent mechanism. Mol. Cell *28*, 121–133.

Lee, K.K., and Workman, J.L. (2007). Histone acetyltransferase complexes: one size doesn't fit all. Nat. Rev. Mol. Cell Biol. *8*, 284–295.

Legube, G., McWeeney, S.K., Lercher, M.J., and Akhtar, A. (2006). X-chromosome-wide profiling of MSL-1 distribution and dosage compensation in Drosophila. Genes Dev. *20*, 871–883.

Lucchesi, J.C., Kelly, W.G., and Panning, B. (2005). Chromatin remodeling in dosage compensation. Annu. Rev. Genet. *39*, 615–651.

Marin, I. (2003). Evolution of chromatin-remodeling complexes: comparative genomics reveals the ancient origin of "novel" compensasome genes. J. Mol. Evol. *56*, 527–539.

Megee, P.C., Morgan, B.A., Mittman, B.A., and Smith, M.M. (1990). Genetic analysis of histone H4: essential role of lysines subject to reversible acetylation. Science *247*, 841–845.

Mendjan, S., and Akhtar, A. (2006). The right dose for every sex. Chromosoma *116*, 95–106.

Mendjan, S., Taipale, M., Kind, J., Holz, H., Gebhardt, P., Schelder, M., Vermeulen, M., Buscaino, A., Duncan, K., Mueller, J., et al. (2006). Nuclear pore components are involved in the transcriptional regulation of dosage compensation in Drosophila. Mol. Cell *21*, 811–823.

Morales, V., Straub, T., Neumann, M.F., Mengus, G., Akhtar, A., and Becker, P.B. (2004). Functional integration of the histone acetyltransferase MOF into the dosage compensation complex. EMBO J. *23*, 2258–2268.

Park, Y., Kelley, R.L., Oh, H., Kuroda, M.I., and Meller, V.H. (2002). Extent of chromatin spreading determined by roX RNA recruitment of MSL proteins. Science *298*, 1620–1623.

Parkinson, H., Kapushesky, M., Shojatalab, M., Abeygunawardena, N., Coulson, R., Farne, A., Holloway, E., Kolesnykov, N., Lilja, P., Lukk, M., et al. (2007). ArrayExpress–a public database of microarray experiments and gene expression profiles. Nucleic Acids Res. *35*, D747–D750.

Schubeler, D. (2006). Dosage compensation in high resolution: global up-regulation through local recruitment. Genes Dev. *20*, 749–753.

Shogren-Knaak, M., Ishii, H., Sun, J.M., Pazin, M.J., Davie, J.R., and Peterson, C.L. (2006). Histone H4–K16 acetylation controls chromatin structure and protein interactions. Science *311*, 844–847.

Smith, E.R., Pannuti, A., Gu, W., Steurnagel, A., Cook, R.G., Allis, C.D., and Lucchesi, J.C. (2000). The drosophila MSL complex acetylates histone H4 at lysine 16, a chromatin modification linked to dosage compensation. Mol. Cell. Biol. *20*, 312–318.

Smith, E.R., Allis, C.D., and Lucchesi, J.C. (2001). Linking global histone acetylation to the transcription enhancement of X-chromosomal genes in Drosophila males. J. Biol. Chem. *276*, 31483–31486.

Smith, E.R., Cayrou, C., Huang, R., Lane, W.S., Cote, J., and Lucchesi, J.C. (2005). A human protein complex homologous to the Drosophila MSL complex is responsible for the majority of histone H4 acetylation at lysine 16. Mol. Cell. Biol. *25*, 9175–9188.

Straub, T., and Becker, P.B. (2007). Dosage compensation: the beginning and end of generalization. Nat. Rev. Genet. *8*, 47–57.

Taipale, M., Rea, S., Richter, K., Vilar, A., Lichter, P., Imhof, A., and Akhtar, A. (2005). hMOF Histone Acetyltransferase Is Required for Histone H4 Lysine 16 Acetylation in Mammalian Cells. Mol. Cell. Biol. *25*, 6798–6810.

Worby, C., Simonson-Leff, N., and Dixon, J.E. (2001). RNA interference of gene expression (RNAi) in cultured Drosophila cells. Sci. STKE *1*, 95.

Wysocka, J., Swigut, T., Milne, T.A., Dou, Y., Zhang, X., Burlingame, A.L., Roeder, R.G., Brivanlou, A.H., and Allis, C.D. (2005). WDR5 associates with histone H3 methylated at K4 and is essential for H3 K4 methylation and vertebrate development. Cell *121*, 859–872.

Yang, X.J., and Seto, E. (2007). HATs and HDACs: from structure, function and regulation to novel strategies for therapy and prevention. Oncogene *26*, 5310–5318.

Zhou, S., Yang, Y., Scott, M.J., Pannuti, A., Fehr, K.C., Eisen, A., Koonin, E.V., Fouts, D.L., Wrightsman, R., Manning, J.E., et al. (1995). Male-specific lethal 2, a dosage compensation gene of Drosophila, undergoes sex-specific regulation and encodes a protein with a RING finger and a metallothionein-like cysteine cluster. EMBO J. *14*, 2884–2895.